2.3. Garrido-Franco, M., Laber, B., Huber, R. and Clausen, T. (2002). Enzyme-ligand complexes of pyridoxine 5'-phosphate synthase: implications for substrate binding and catalysis. *J. Mol. Biol.* (Submitted).

Journal of Molecular Biology

Enzyme-Ligand Complexes of Pyridoxine 5'-Phosphate Synthase: Implications for Substrate Binding and Catalysis

Marta Garrido-Franco, Bernd Laber[1], Robert Huber and Tim Clausen[*]

Max-Planck-Institut für Biochemie, Abteilung Strukturforschung, D-82152 Planegg-Martinsried, Germany

[1]Aventis CropScience GmbH, Forschung Biochemie, D-65926 Frankfurt am Main, Germany

[*]Corresponding author, Tel. +49-89-8578 2680, Fax +49-89-8578 3516, email: clausen@biochem.mpg.de

Running Title

Mode of Action of PNP Synthase

Abbreviations

AAP, 1-amino-acetone-3-phosphate; DXP, 1-deoxy-D-xylulose-5'-phosphate; GAP, glycerolaldehyde-3-phosphate; P_i, inorganic phosphate; PLP, pyridoxal 5'-phosphate; PMP, pyridoxamine 5'-phosphate; PNP, pyridoxine 5'-phosphate.

Key Words

Enzyme-substrate complex, Open-closed transition, PdxJ, PLP, Vitamin B_6

SUMMARY

Pyridoxine 5'-phosphate (PNP) synthase is the last enzyme in the *de novo* biosynthesis of vitamin B_6 catalyzing the complicated ring-closure reaction between 1-deoxy-D-xylulose-5'-phosphate and 1-amino-acetone-3-phosphate. Here we present the crystal structures of four PNP synthase complexes with substrates and substrate analogues. While the overall fold of the enzyme is conserved in all complexes, characteristic readjustments were observed in the active site. The complementary structural information allowed us to postulate a detailed reaction mechanism. The observed binding mode of substrates indicates how the first reaction intermediate, the Schiff-base conjugate, is formed. The most important mechanistic features are the presence of two phosphate-binding sites with distinct affinities and the existence of a water relay system for the release of reaction waters. Furthermore, the complexes provide the basis to rationalize the open-closed transition of a flexible loop located on the C-terminal side of the TIM-barrel. Binding of both substrate molecules to the active site seems to be a prerequisite to trigger this transition. Highly conserved mechanistically important residues in the PNP synthase family imply a similar active site organization and reaction mechanism for all family members. Due to the exclusive presence of PNP synthase in a subset of eubacteria, including several well-known pathogens, and due to its outstanding physiological importance for these organisms, the enzyme appears to be a promising novel target for antibacterial drug design.

INTRODUCTION

The biocatalytically active form of vitamin B_6, pyridoxal 5'-phosphate (PLP) acts as enzymatic cofactor in a multitude of amino acid transformations. The related B_6 vitamer, pyridoxamine 5'-phosphate (PMP), is involved in the metabolism of deoxysugars. Whereas most microorganisms and plants synthesize vitamin B_6 *de novo*, the corresponding biosynthetic machinery is absent in mammals. They have to obtain at least one of the B_6 vitamers from their diet and can afterwards interconvert them into each other by the so-called salvage pathway (for a review see Spenser and Hill (1995)[1]). The enzymatic apparatus of *de novo* vitamin B_6 biosynthesis is by far best characterized in *E. coli,* with four *pdx* proteins specifically involved.[2-6]

Pyridoxine 5'-phosphate (PNP) synthase (also referred to as PdxJ) catalyzes the terminal step in *E. coli de novo* vitamin B_6 biosynthesis, the condensation of 1-deoxy-D-xylulose-5'-phosphate (DXP) and 1-amino-acetone-3-phosphate (AAP) yielding pyridoxine 5'-phosphate (PNP), inorganic phosphate (Pi) and two water molecules.

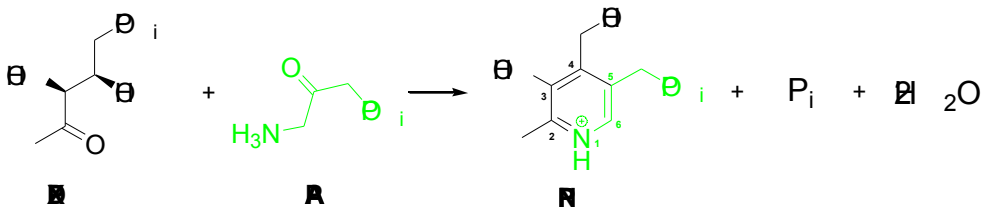

However, not all organisms that synthesize vitamin B_6 have equivalents of the *E. coli* *pdx* genes. Recently it could be demonstrated that two autoexclusive anabolic routes exist. In fungi, plants, archeobacteria and some eubacteria, the *SOR1* gene product (singulet oxygen resistance) has been identified to be the central biosynthetic enzyme.[7-10]

In contrast, the *pdx* family is restricted to eubacteria. Among the species that express PNP synthase are some prominent pathogens like *Bordetella bronchisepticum*, *Helicobacter pylori*, *Neisseria gonorrhoeae*, *Neisseria meningitidis*, *Salmonella typhi*, *Salmonella typhimurium, Vibrio cholerae* and *Yersinia pestis*, and for them PNP synthase appears to be of outstanding physiological importance as deduced from its high degree of conservation. This makes PNP synthase and interesting pharmaceutical target for novel antibacterial agents with the inherent potential to tackle the increasing problem of antibiotic resistance.

As a first step towards rational drug design, we have previously determined[11] the crystal structure of *E. coli* PNP synthase. The quaternary structure of the enzyme is the octamer, which is organized as a tetramer of dimers. The monomer is comprised of one compact domain showing the frequently observed TIM-barrel fold. Three "extra"-helices respective to the basic $(\beta/\alpha)_8$ architecture mediate the intersubunit contacts. The active unit of the oligomer is the dimer, as indicated by the formation of shared active sites: Arg20 from one monomer protrudes to the active site of the partner subunit where it is directly involved in substrate binding. The most outstanding mechanistic feature is a flexible loop that closes the active site upon substrate binding.

Here we present four refined crystal structures of PNP synthase from *E. coli* in complex with substrates, substrate analogues and phosphate. The new structural information provides novel insights in the mechanism of active site closure and highlights the residues essential for catalysis. These new functional data are paramount to an understanding of the complex catalytic mechanism of PNP synthase.

RESULTS AND DISCUSSION

Model quality and structure description

The structures of all complexes were refined by standard procedures implemented in CNS[12]. As starting model the uncomplexed PNP synthase was used (PDB accession code 1HO1) in which all water molecules were omitted.

The structural models herein presented comprise the following complexes: a so-called enzyme-substrate complex with DXP and glycerolaldehyde-3-phosphat (GAP), a complex with GAP as substrate analogue, and two complexes with inorganic phosphate, in which crystals were either soaked with a 100 mM or a 10 mM phosphate solution (Fig.1). The crystal structures of the complexes are of high quality as indicated by the stereochemical and refinement statistics (Table 1). In a Ramachandran plot, the protein backbone torsion angles for 93.5 to 94.4 % residues fall in the most favored regions, 5.6 to 6.5 % fall in additional allowed regions and only up to 0.3 % fall in generously allowed regions. His193 is the only Ramachandran outlier. His193 is an active site residue that is directly involved in anchoring the phosphate of the incoming substrate. Remarkably, this residue is an outlier in the ES, EPi2 and EA complexes, whereas the torsion angles in the uncomplexed, EPi1 and EP structures fall within the energetically allowed regions. As discussed later, this difference seems to be important for the open-closed transition. All PNP synthase complex structures share the secondary and tertiary structure of the native enzyme. Largest differences between the individual structures arise by distinct conformations of loop 4 that closes the active site upon substrate binding.

Furthermore, residues that directly interact with the bound ligands exhibit characteristic variations in the positioning of their side chains.

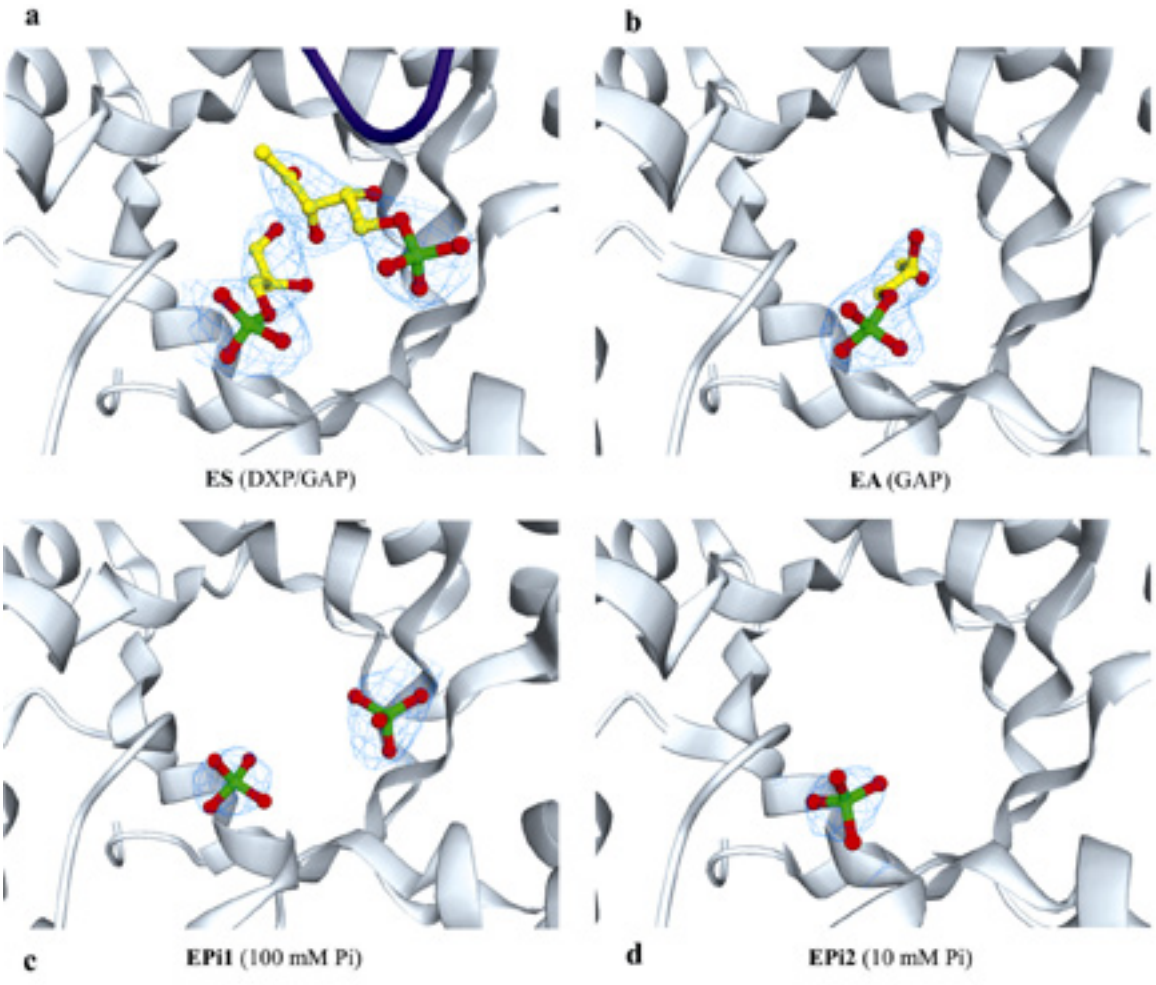

Figure 1 Refined complex structures of PNP synthase. In all cases, the omit map (omitting the bounds ligands) was calculated at 2.3 Å resolution and contoured at 3.0 _. The carbon atoms of the ligands are shown in yellow and the phosphate in green. **a** Enzyme-substrate complex (ES). The phosphate groups of both GAP and DXP represent the main anchor to the active site, binding at the P1 and P2 site, respectively. After substrates bind, loop 4 (violet) closes the active site. **b** Enzyme-substrate analogue complex (EA). Here, the GAP molecule is bound in identical manner as in the ES complex. **c** Enzyme-phosphate complex 1 (EPi1). When the crystals were soaked in a 100 mM phosphate buffer solution, two phosphate molecules were observed in the active site. **d** Enzyme-phosphate complex 2 (EPi2). When the crystals were soaked in a 10 mM phosphate buffer solution, only a single phosphate was found in the active site, at P1. These figures and Fig.5 were produced with MOLSCRIPT[21] and RASTER3D[22].

	DXP/GAP (ES)	Pi (EPi1)	Pi (EPi2)	GAP (EA)
Data collection				
Soaking solution (mM)	2.5/2.5	100	10	20
Resolution (Å)	25.0 – 2.3	25.0 – 2.3	25.0 – 2.3	25.0 – 2.3
Cell parameters (Å)	a=128.9	a=132.0	a=130.9	a=129.8
	b=156.3	b=154.8	b=155.4	b=155.9
	c=127.6	c=130.4	c=129.0	c=127.4
Reflexions				
observed	165,177	190,793	198,531	187,532
unique	53,504	55,933	58,001	57,133
R_{merge}[a]				
overall	7.9	12.3	4.5	5.0
outher shell	46.4	38.1	34.3	22.0
I/I(_)				
overall	9.2	5.7	13.4	12.2
outher shell	1.6	1.7	2.2	2.7
Completeness				
overall	93.8	94.6	99.8	99.8
outher shell	90.4	89.2	99.2	99.4
Refinement				
Active atoms	8,157	7,882	7,449	7,474
protein/solvent/ligand	7,340/727/90	7,298/544/40	7,096/333/20	7,098/328/50
Averaged B	33.2	52.7	28.4	44.4
protein/solvent/ligand	32.8/34.4/45.4	52.9/48.6/86.4	28.2/28.1/81.0	44.2/65.2/40.2
r.m.s.d.				
bonds/angles/bonded B's	0.011/1.75/2.7	0.009/1.44/2.8	0.009/1.46/1.4	0.009/1.46/1.2
R_{factor}[b] (R_{free})[c] %	18.0 (22.4)	21.0 (26.6)	22.1 (27.0)	22.0 (26.0)

[a] $R_{merge}=\sum_{hkl}| I - I|/\sum_{hkl}|I|$

[b] $R_{factor}=\sum_{hkl}||F_{obs}| - |F_{calc}||/\sum_{hkl}|F_{obs}|$

[c] R_{free} is the R-value calculated with 5% of the data that were not used for the refinement.

Table 1 Data collection and refinement statistics.

Binding of the substrate

As analog of AAP we used GAP. The lack of the amino group at C3 prevents the reaction to proceed. The resulting ternary complex may serve as a model for the ES complex PdxJ-DXP-AAP. Therefore, we refer to this complex as the ES complex. In addition to the EP complex[11], the ES complex was helpful to compare the binding mode of substrates and products and to detect structural differences of mechanistically relevant

active site residues. The DXP and GAP molecules are well ordered in the active site and their binding affected neither the crystal packing nor the diffraction quality of the soaked crystals, which diffracted up to 2.3 Å resolution. Unambiguous F_o-F_c density allowed modeling of both ligands in each of the four monomers of the asymmetric unit. Upon substrate binding, loop 4, the most flexible part in the structure is observed in all four PNP subunits closed upon the active site thereby sequestering the substrates from the outside. In contrast, in the EP complex, all four subunits display different conformations of loop 4 corresponding to an open, a closed and an intermediate state of PNP synthase. Active site closure provides an adequate environment to exclude possible secondary reactions and to stabilize reaction intermediates. Superimposing the ES main-chain atoms on those of the uncomplexed enzyme, the average root mean square (r.m.s.) deviation of 235 structurally equivalent C^{α} atoms was 0.34 Å excluding residues 97-103 of loop 4. Loop 4 swings into the active site whereby Thr103 exhibits the largest movement of 15.7 Å. In the ES complex, loop 4 is directly involved in substrate binding. Two of its residues, Thr102 and Thr103, are participating in the hydrogen-bonding network around the DXP molecule, interacting with its phosphate and 4-OH group (Fig.2a). In the ternary ES complex (Fig.1a), the substrate DXP and the substrate-analogue GAP are mainly anchored in the active site by their respective phosphate groups. To distinguish both phosphate-binding sites and following the EP nomenclature, we refer to the GAP derived site as the P1-site (corresponding to the PNP P1-site) and to the DXP-site as the P2-site. Similarly to the EP complex (Fig.2b), residues from loop 7 and loop 8 mediate the interactions between the enzyme and GAP by binding tightly its phosphate group. Further

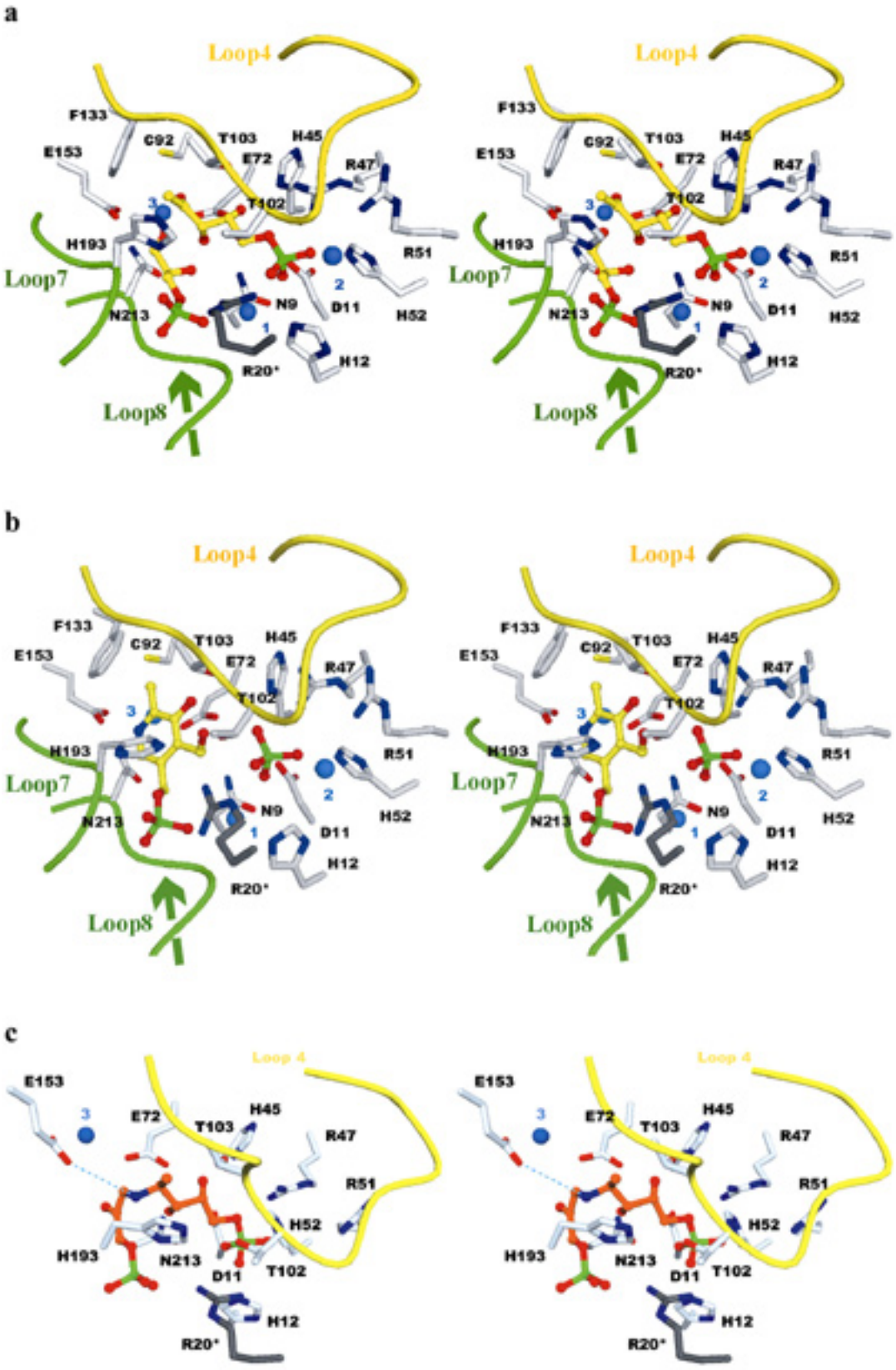
a
Loop4
F133
C92
T103
H45
E153
E72
R47
T102
3
H193
R51
Loop7
2
N9
D11
H52
N213
1
H12
R20*
Loop8
Loop4
F133
C92
T103
H45
E153
E72
R47
T102
3
H193
R51
Loop7
2
N9
D11
H52
N213
1
H12
R20*
Loop8
b
Loop4
F133
C92
T103
H45
E153
E72
R47
T102
3
H193
R51
Loop7
2
N9
H52
D11
N213
1
H12
R20*
Loop8
Loop4
F133
C92
T103
H45
E153
E72
R47
T102
3
H193
R51
Loop7
2
N9
H52
D11
N213
1
H12
R20*
Loop8
c
Loop 4
E153
3
E72
T103
H45
R47
R51
H52
H193
N213
D11
T102
H12
R20*
Loop 4
E153
3
E72
T103
H45
R47
R51
H52
H193
N213
D11
T102
H12
R20*

Figure 2 Binding in the active site of PNP synthase. **a** Detailed stereoview of the ES complex. For clarity, the carbon atoms of DXP and AAP and the C$^-$ trace of loop 4 are shown in yellow, water molecules are shown as blue balls, and the backbone of the P1 binding site constructed by loops7 and 8 is shown in green. The macrodipole of helix 8a is indicated as an arrow. **b** Detailed stereoview of the EP complex. The colors are as indicated in a. **c** Model of the initial Schiff base conjugate. The carbon atoms of the Schiff base intermediate are colored orange, the C$^-$ backbone of loop 4 is shown in yellow, and the active site water in cyan. Note that Glu72 and Glu153 are in close contact to the Schiff base nitrogen. Residues surrounding the Schiff base intermediate are indicated. These figures, as well as Fig.6b, were created with DINO (http://www.bioz.unibas.ch/~xray/dino).

anchoring is achieved by the macrodipole of helix 8a and by ionic interactions with Arg20*. The DXP substrate is also firmly positioned by its phosphate group. Hydrogen bonds are formed between the DXP phosphate and Arg20*, Asp11, His12, Arg47, His52 and two residues from the "closed" loop 4: Thr102 and Thr103 (Fig.2a). Especially Arg20* and Arg47 are involved in charge compensation of DXP phosphate as deduced from their close distance. Finally, two well-defined water molecules are observed in hydrogen-bonding distance to both phosphate groups, water 1 is wedged between them and water 2 is bound to the DXP phosphate at the P2-site. A hydrogen bond network involving the side chains of Asn9, His45, Glu72, Thr103 and Glu153 achieves further binding of the two ligands DXP and GAP as indicated in Fig.2a. The observed complex with DXP and GAP suggests that the protein orients the substrate molecules properly for Schiff-base formation between the DXP carbonyl and the AAP amino group. The presence of continuous electron density between DXP and GAP at the corresponding position motivated us to model the Schiff base. The model indicates how this first reaction intermediate might be positioned and stabilized by Glu72 and Glu153 in the active site (Fig.2c) and is consistent with results of the EP complex, where both glutamates are in close contact to the protonated nitrogen of the pyridine ring.

Furthermore, the modeling confirms our prediction that the P2 site is only accessible for the DXP-phosphate before condensation and for the subsequently formed inorganic phosphate.

Complexes with inorganic phosphate

Structure determination of PNP synthase in complex with inorganic phosphate was performed to investigate the affinity and specificity of the two phosphate-binding sites and to analyze the effect of phosphate binding on the conformation of loop 4; i.e. if phosphate binding is sufficient to trigger active site closure. In a crystal soaked with 100 mM phosphate solution (EPi1) we could see positive electron difference density localized at both the P1 and P2 sites (Fig.1c), where two phosphate molecules could be refined in each of the four monomers (average B-factor of 86.4 $Å^2$). In all monomers loop 4 was well defined in its open state (B-factor of 45 $Å^2$ for D and 75 $Å^2$ for A, B, C). The two phosphates are bound to the protein by a similar hydrogen-bonding network as observed in the ES complex. Arg20* is involved in binding of both phosphate ligands. At the P1-site, the side-chain of His193 and the main-chain amides of Gly194, Gly215 and His216 achieve binding, whereas binding at the P2-site is established by the side-chains of Asp11, His12, Arg51 and His52. When the phosphate concentration of the soaking solution was reduced 10-fold to 10 mM (EPi2), only the P1 site was occupied by phosphate (Fig.1d) and the electron density of loop 4 was not defined. Referring to the active site waters in ES, EPi1 and EPi2 only water 1 is conserved. Water 2, which is bound to the DXP phosphate, is absent in EPi2 and in EPi1. Moreover, water molecules in the phosphate complexes occupy characteristic binding sites of ES and EP complex.

We propose that the P1 site, which corresponds to the PNP (EP) and GAP (ES) phosphate binding site, has a stronger affinity for phosphate than P2. Most probably this difference arises by the contribution of helix 8a macrodipole to the P1 site. A similar situation was observed in one of the monomers of the EP complex, where the inorganic phosphate bound at the P2-site had already left the active site while the PNP molecule was still anchored at the P1-site. The two phosphate complexes also indicate that their binding is not sufficient for active site closure and specific interactions with other parts of the substrates are required.

Complex with a substrate-analogue

To better understand the loop 4 closure, we tried several soaks with DXP and the AAP analogues GAP and 4-aminobutylphosphonic acid (4-ABP). While crystals soaked with DXP and 4-ABP were not diffracting, we succeeded to determine the structure of the PNP synthase GAP complex. This complex mimics the situation when only AAP is bound to the active site.

Superposition with the ES complex resulted in a r.m.s. deviation of 0.25 Å for 234 residues and superposition with the native structure yields a r.m.s. deviation of 0.19 Å for 235 C^{-} atoms. Only residues directly contacting the GAP molecule undergo slight readjustments upon complex formation. The electron density of the GAP ligand in the active site could be unambiguously interpreted allowing its precise allocation. The GAP molecule was bound in identical manner as observed in the ES complex: Its phosphate is fixed at the P1-site by the main chain amides of residues Gly194, Gly215 and His216. Further interactions are with residues Asn9, Glu72, His193 and Arg20* (Fig.1b).

Remarkably in all monomers of the asymmetric unit, residues 97-103 of the flexible loop 4 are not defined by electron density indicating to an increased mobility of loop 4 in this complex.

Active site closure upon substrate binding

Regarding the location of the mobile loop 4, E and EPi1 occur in the open form, while ES is present in the closed state. Moreover, in the EP complex both states are present, but in EA and EPi2 loop 4 is not defined. The superposition of the different structures (Fig.3) illustrates the most characteristic structural changes and suggests a likely mechanism for the open-closed transition. Largest differences during this conversion are observed for loop 4 that is folded away from the active site in the open form, but reorientates upon interaction with proper ligands and buries the active site. The distribution of thermal motion factors indicates that those residues of loop 4, which reorient, have an increased mobility in the crystal. We propose that in the free enzyme loop 4 alternates between the open and closed position as suggested by the observation of different conformers in the uncomplexed enzyme. Upon substrate binding to the open active site, loop 4 rearranges by changes in the φ- and ϕ-angles of the "hinge" residues Glu96 ($\Delta\phi$=160°) and Gly106 ($\Delta\varphi$=150°, $\Delta\phi$=50°). The bordering residues of loop 4, i.e. those before Glu96 and after Gly106, and the side-chain of Glu96 itself are firmly anchored to the core of the TIM-barrel. The hydrogen-bonding network extending from the flexible part of loop 4 in the closed form has the appearance of a zipper embedding substrates and reaction intermediates in the active site of PNP synthase. Closure of this active-site zipper seems to be a concerted process that should start at the N-terminal end of loop 4. We propose that Arg47 swings down to hydrogen bond with the DXP phosphate, thereby triggering

the open-closed transition. The guanidino group of Arg47 moves around 3.5 Å and fixes the side-chain of the flexible Glu100 that in turn strongly interacts with the amide nitrogen of hinge residue Glu96 and stabilizes its "closed" conformation. The backbone of residues 96 – 103 flips inward and successively hydrogen bonds are formed between Arg98(O)-Arg51, Glu100(O)-Arg51, Val101(O)-Arg51, Thr102-DXP(phosphate), Thr103-DXP(4'OH) and Glu104(O)-His193. At the opposite end of loop4, the two glycine residues Gly105 and Gly106 allow sufficient backbone flexibility to complete the transition (Fig.3a). Binding of two single phosphate ions at the P1- and P2-sites does not lead *per se* to a conformational change. The observed structural differences between ES and both EP forms may reflect the scenario that triggers active-site reopening. The unlocking should proceed by reversing the sequence of events that resulted in active-site closure and thus start at the C-terminal end of loop 4. Consistently, loss of the hydrogen bond between His193 and Glu104 carbonyl is observed in the closed EP form. Further destabilization of the closed state may be achieved by disruption of the interaction between PNP-4'OH and Thr102-OH as seen in the open EP complex.

Comparison of the ES, EPi1, EPi2 and EA structures indicate another notable feature, which is correlated with His193 and its two preceding residues (Fig.3b). Differences in this region directly influence the conformation of loop 4. Destabilization of the closed state seems to be the consequence of the disruption of the hydrogen bonds between Thr102-His193 and Thr103-PNP. The interaction of His193 either with Thr102 or Thr103 depends on the orientation of the histidine ring, which in turn depends on the backbone conformation of residues 191-193. Structural comparison suggests that the open-closed transition is associated with a peptide flip. The peptide bond between Ala191

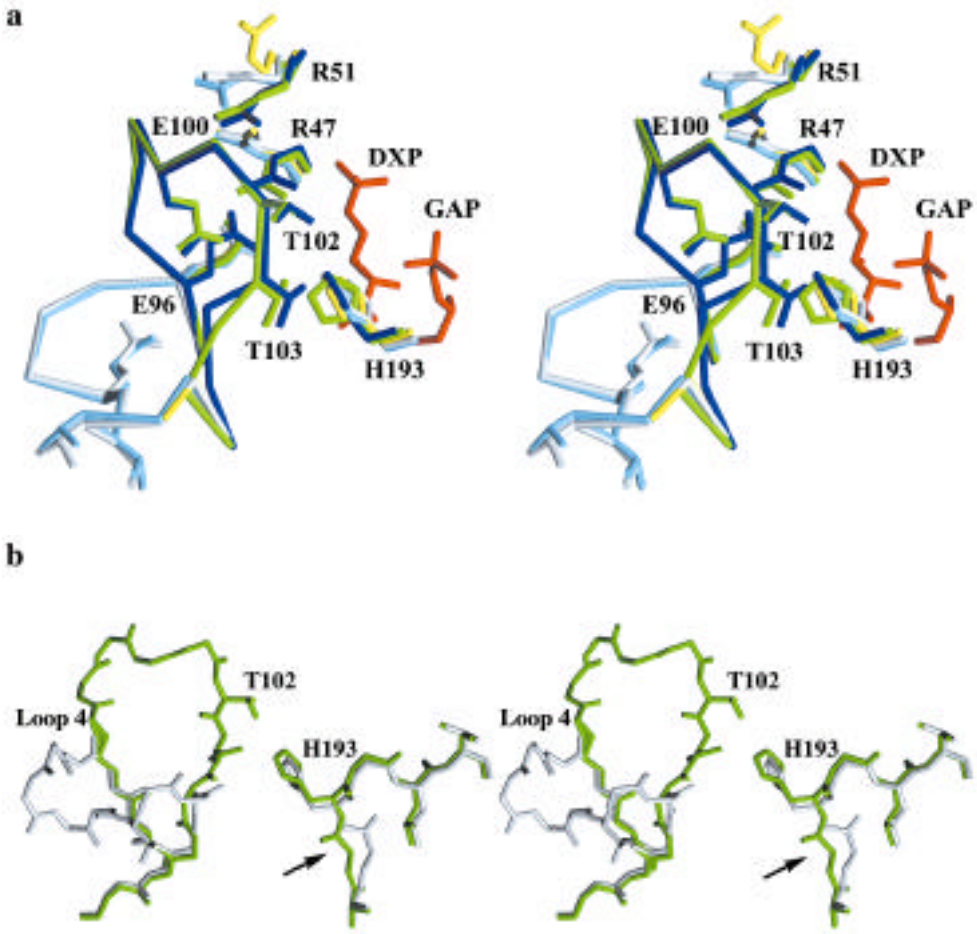

Figure 3 Open-closed transition. **a** Stereoview representation of residues that undergo positional changes between the different complexes. The structures with an open loop 4 conformation are the native (grey) and the EPi1 complex (cyan), in the EA complex (yellow), loop 4 is not defined and in the ES (green) and EP (blue) complexes, their loop 4 is in the closed conformation. In order to clarify the situation of the active site, the DXP and GAP substrates are highlighted in red. **b** Detailed drawing of the peptide flip. The colour code is as in **a**. For clarity, the EA and EPi complexes were not included. The situation in EPi1 is identical to the native state. In the EPi2 and the EA complexes, loop 4 is not defined. The peptide bond between Ala191 and Ala192 is indicated with an arrow. These figures were created with SETOR[23].

and Gly192 adopts main-chain conformational angles Ψ(Ala191) = 163°, Φ(Gly192) = 159° in the open form, compared to Ψ(Ala191) = -40°, Φ(Gly192) = 134°, in the closed form. In cases where loop 4 is not defined (EPi2 and EA complexes), both peptide conformations appear to be present. Consistently, the B-factors of the atoms of the

corresponding peptide increase from about 25 $Å^2$ to 50 $Å^2$. Thus the peptide flip, which is directly related with the energetically disfavored Ramachandran outlier His193 in the closed forms, might represent a trigger for the closed-open transition. Remarkably, residues 191-194 are strictly conserved in the PNP synthase family.

Proposed reaction mechanism

Several mechanistic proposals have been put forward to how PNP synthase catalyzes the complex multistep reaction of PNP formation which involves Schiff base formation, water elimination and addition, P_i elimination, ring closure and various proton shifts.[5,6,13] However, especially the sequence and timing of the individual steps remained a matter of speculation. Based on the active site structures of native and complexed PNP synthase the following molecular reaction mechanism for the synthesis of PNP is proposed. The scheme in Fig.4 indicates how interactions between active site residues and ligands can stabilize intermediates during the catalytic cycle. The observed conformational changes are expected to occur after initial binding of both substrates (open – closed, **I**) and after release of P_i (closed – open, **IV**).

In the Michaelis complex **I**, both substrates are anchored mainly by their respective phosphate groups. While the central element in binding the AAP phosphate is the macrodipole of helix 8, the phosphate group of DXP is fixed at a highly basic groove constructed by three histidines, three arginines and one aspartate. Further binding is achieved by the interaction of the DXP hydroxylic groups with Glu72 and Thr103, by van-der-Waals interactions between the DXP C1-methyl group and Phe133, and by a hydrogen-bond between Asn9 and the AAP carbonyl oxygen. In concert, these

interactions properly position the substrates for Schiff base formation. As already mentioned His45, Glu72, Glu153 and water 3 set up a charge and proton relay system. Our criteria to specify which one of those residues acts in each step are based on the observed interatomic distances (Table 2). We suggest that both Glu72 and Glu153 are unprotonated. His45 may also be unprotonated in the vicinity of Arg47. Most probably

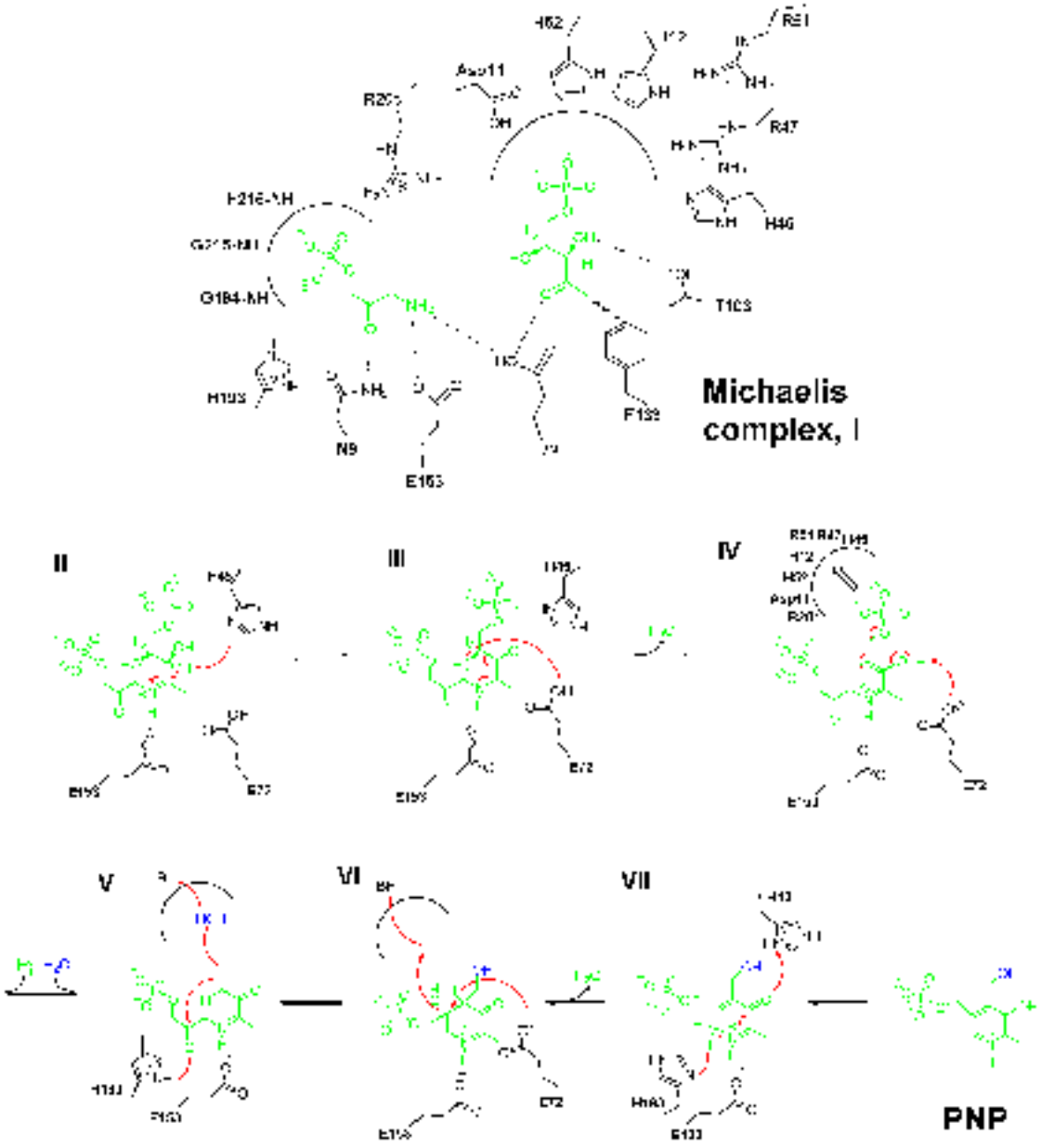

Figure 4 Proposed mechanism for PNP synthase. Indicated are the relevant reaction intermediates (**I - VII**).

Glu72 initiates the reaction by deprotonating the AAP amino group, thereby enabling its nucleophilic attack at the DXP carbonyl carbon and Schiff base formation. After release of a water molecule the carboxylate group of Glu153 stays in close contact to the aldimine nitrogen in order to stabilize the protonated Schiff-base intermediate that develops during the catalytic cycle.

	ES		**EPi1**		**EPi2**		**EA**	
Asn9-ND2	DXP-O3	(3.5)	-		-		GAP-O1	(2.8)
	GAP-O2	(2.8)						
Asp11-OD2	DXP-OP3	(2.8)	P_i2-OP3	(2.6)	-		-	
His12-ND1	DXP-OP1	(3.9)	-		-		-	
	-OP2	(3.0)						
-NE2	-		P_i2-OP2	(3.9)	-		-	
His45-NE2	DXP-O4	(2.6)	-		-		-	
-ND1	-		P_i2-OP2	(3.6)	-		-	
Arg47-NH1	DXP-OP1	(2.4)	-		-		-	
His52-NE2	DXP-OP1	(2.9)	P_i2-OP2	(2.9)	-		-	
Glu72-OE1	DXP-O2	(3.3)	P_i2-OP2	(4.5)	-		-	
	-O3	(2.9)						
	-O4	(2.7)						
-OE2	GAP-O1	(2.4)	-		-		GAP-O1	(2.8)
	-O2	(3.4)					-O2	(3.9)
Thr102-OG1	DXP-OP2	(3.1)	-		-		-	
Thr103-OG1	DXP-O4	(3.4)	-		-		-	
Glu153-OE1	DXP-O2	(4.4)	-		-		GAP-O1	(5.0)
	GAP-O1	(3.0)[b]						
His193-ND1	GAP-OP3	(2.9)	P_i1-OP3	(3.7)	P_i1-OP3	(3.4)	GAP-O2	(3.4)
Gly194-N	GAP-OP3	(2.7)	P_i1-OP3	(2.6)	P_i1-OP3	(3.3)	GAP-OP3	(2.8)
					-OP2	(3.6)		
Gly215-N	GAP-OP3	(2.9)	P_i1-OP3	(3.5)	P_i1-OP2	(2.6)	GAP-OP3	(2.7)
	-O2	(4.9)	-OP4	(3.2)	-OP4	(2.7)	-OP4	(3.4)
His216-N	GAP-OP4	(2.8)	P_i1-OP4	(2.7)	P_i1-OP4	(2.7)	GAP-OP4	(2.5)
	-O2	(4.7)						
Arg20*-NH1	DXP-OP1	(2.6)	P_i1-OP2	(3.8)	P_i1-OP2	(3.8)	GAP-OP3	(2.5)
	GAP-OP2	(2.5)						
-NH2	DXP-OP2	(2.3)	P_i2-OP2	(3.1)	-		-	

[a] The distances in brackets are given in Å. The table summarizes those residues that enclose the ligands. To indicate differences between the discussed structures, sometimes also distances > 4.0 Å are included.

[b] The corresponding distance in EP (closed) between the Glu153-OE1 and the N of the pyridine is 2.7 Å.

Table 2 Interatomic distances between PNP synthase and bound ligands[a].

In the next part of the reaction (**II**, **III**), in which a second water molecule is released, Glu72 and His45 act as a catalytic unit tuning mutually their individual pK_a's. Upon substrate binding, the negative charge of the incoming DXP phosphate increase the pK_a of His45, which abstracts a proton from DXP-C3. Stabilization of the developing carbanionic intermediate is accomplished by the protonated Schiff base that functions as an electron-sink (**II**). Protonation of the C4-hydroxylic group of DXP is catalyzed by Glu72, which is in hydrogen-bonding distance to His45 and may sense its changed protonation state (**III**).

The elimination of the DXP-P_i from the enzyme-bound enol (**IV**) is initiated by the Glu72 catalyzed deprotonation of the DXP C3-hydroxyl. PNP synthase provides the P_i-binding pocket, formed by Arg20*, Asp11, His12, His45, Arg47, Arg51 and His52 (**IV**). The structures of the PNP synthase EP and ES complexes and the model of the Schiff base conjugate demonstrate that this pocket can only be occupied by the released but not by the DXP-bound phosphate of intermediates **II** and **III**. Protonation of the Glu72 carboxylate and positional rearrangement of His45 upon P_i elimination weakens the interaction of these two residues and triggers rearrangement of loop 4 and thus active-site opening. As discussed before the P_i-affinity is diminished in the open conformation, thus allowing the release of P_i from the active site. We suggest that after P_i release a water molecule is bound in the P_i-binding pocket and is activated by one of the contacting histidines (**V**). Nucleophilic attack of this water molecule at DXP-C5 induces the ring closure reaction between the carbon atoms destined to become C4 and C5 of PNP. The crystal structure indicates that His193 is the only candidate to protonate the AAP carbonyl oxygen. Of great mechanistic importance is the aspect that the side chain of

Glu72 can approach each of the PNP ring atoms which in turn determines its acidity. The close contact to the O3'-carbonyl (2.9 Å) increases the basicity of Glu72. Thus, Glu72 is a likely candidate to initiate hydroxid elimination (**VI**) by abstracting a proton from the C4 carbon. Providing the basic electrostatic potential of the Pi-binding pocket may further facilitate the release of the hydroxide ion. Finally, His193 and His45 catalyze the proton shift from C6 to O3' yielding PNP (**VII**). It should be noted that the order of the proposed reaction steps might be reversed, maintaining the catalytic functions of the participating groups.

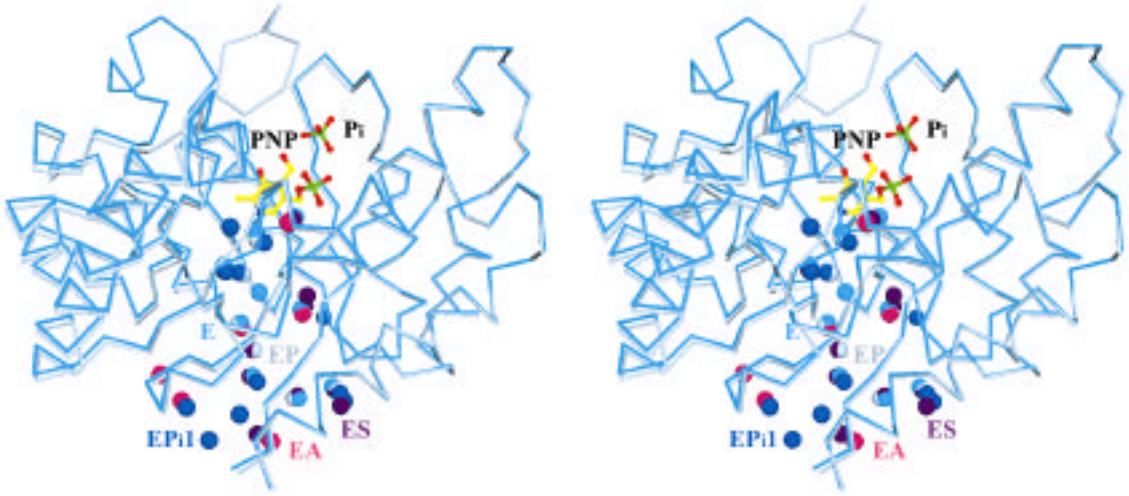

Figure 5 Solvent channel of PNP synthase. The C- backbone of the native (open loop 4) and of the EP complex (closed loop 4) are shown in cyan and gray, respectively, to highlight the position of the central _ core. The shown water molecules where observed in the different complexes and are differentially colored: waters of the native enzyme in cyan, of the EP complex in gray, of the ES complex in violet, of the EPi1 complex in blue, and of the EA complex in magenta.

In a preceding paper[11] we identified a water channel that runs through the center of the _-barrel. This hydrophilic channel seems to be of mechanistic importance. During the reaction catalyzed by PNP synthase three water molecules are formed. These reaction

waters have to be released from the active site. As the entrance of the active site is closed by loop 4 when the reaction takes place, water molecules have to leave by the N-terminal backdoor. Superimposing the native structure with all complexes indicates that not all water positions in the central channel of the TIM barrel are equally occupied (Fig.5). This observation strengthens the proposal of a water-relay system, allowing removal of active site waters.

Conservation of residues between species

A multiple sequence alignment of PNP synthase performed with Alscript[14] reveals that 78 residues (29.5% of the 242 residues in *E. coli* PNP synthase) are strictly conserved, and further 57 residues are strongly conserved (Fig.6a). When the conservation pattern is mapped on the molecular surface of the active dimer (Fig.6b), conserved and variable regions can be clearly distinguished. Half of the strictly conserved residues (39 from 78) are located at the C-terminal end of the _-barrel forming part of the active site wall. Among the strictly conserved residues are most of the residues proposed to be directly involved in substrate binding or catalysis, *e.g.* Arg20, Arg47, Arg51, Glu72, Thr102, Thr103, Glu153, His193. The remaining invariant residues have either structural roles at the monomer-monomer contact interface of the active dimer, or are part of the important loop 4. This conservation pattern implies that organisms such as *Aquifex aeolicus*, *Aquifex pyrophilus*, *Bordetella bronchisepticum*, *Caulobacter crescentus*, *Helicobacter pylori*, *Neisseria gonorrhoeae*, *Neisseria meningitidis*, *Salmonella typhi*, *Salmonella typhimurium*, *Shewanella putrefaciens*, *Synechocystis sp*, *Vibrio cholerae*, and *Yersinia pestis*, should have strikingly similar active site architectures and follow the same

mechanistic route as the *E. coli* enzyme. Among the bacterial species that express PNP synthase are several well-known pathogens. Coming structural studies will therefore concentrate on the modelling of novel inhibitors of PNP synthase. The wealth of the presented structural information should facilitate this process.

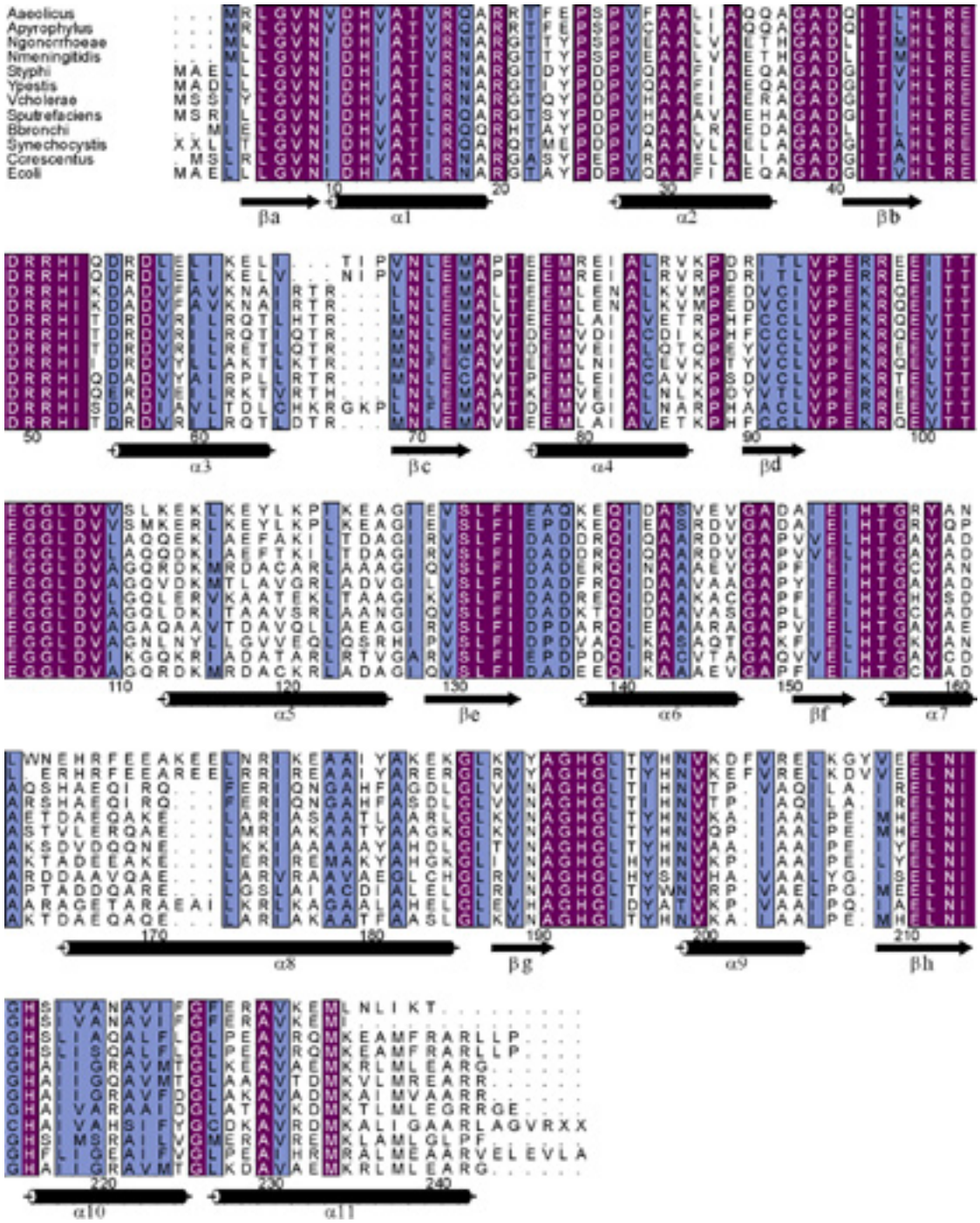

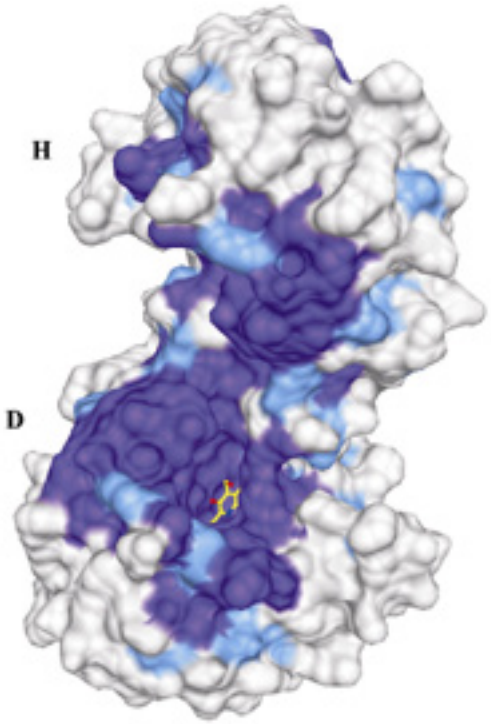

Figure 6 Conservation pattern in the PNP synthase family. **a** Amino acid sequence alignment of PNP synthase from twelve different organisms. Strictly conserved residues are coloured in purple and highly conserved residues in cyan. Numbering and secondary structure of the *E.coli* protein are given. The alignment was produced with the GCG Wisconsin package (Version 9.1, Genetics Computer Group, Madison) and Alscript[14]. Abbreviations used are Aaeolicus, *Aquifex aeolicus*; Apyrophilus, *Aquifex pyrophilus* ; Ngonorrhoeae, *Neisseria gonorrhoeae*; Nmeningitidis, *Neisseria meningitidis*; Styphi, *Salmonella typhi*; Ypestis, *Yersinia pestis*; Vcholerae, *Vibrio cholerae*; Sputrefaciens, *Shewanella putrefaciens*; Bbronchi, *Bordetella Bronchisepticum*; Synechocystis, *Synechocystis sp.*; Ccrescentus, *Caulobacter crescentus*; Ecoli, *Escherichia coli*. **b** Surface of the active dimer with bound PNP in the open form. The results from the sequence alignment were mapped on the solid surface to demonstrate the high degree of conservation of loop 4, the active site region and the intersubunit interfaces.

MATERIAL AND METHODS

Crystallization and data collection

PNP synthase was purified and crystallized as previously reported[6,15]. Diffraction data up to 2.3 Å for the ES, EPi1 EPi2 and EA complexes were collected at our in-house Mar

Research (Hamburg, Germany) image plate system mounted on a Rigaku (Tokyo, Japan) rotating anode generator operated at 50kV/100mA with CuK_α radiation (λ=1.5418 Å). Best results were obtained by incubating PNP synthase native crystals for 4 hours in 2.5 mM DXP / 2.5 mM GAP, 3 hours in 10 mM and 100 mM phosphate and for 3 days in 20 mM GAP. The unit cell parameters of the complexes were slightly different but still isomorphous with the native form (Table 1). Processing of the diffraction data and scaling of the individual structure factors sets were performed with programs of the hkl suite[16] and the CCP4 package[17] respectively.

Structure determination and refinement

The native structure was used as the starting model for the determination of all complexes. After a first rigid body protocol using the program CNS[12], the resulting models were submitted to various cycles of positional and B-factor refinement. For energy-restrained structure refinement, maximum likelihood algorithms implemented in CNS[12] and the protein parameters of Engh and Huber[18] were used. Model building was done with the program O[19]. In later stages, solvent molecules were introduced at stereochemically reasonable positions with high difference electron densities. Ligands were only included in the last round of refinement. The statistics for the final refinement state of all complexes is shown in Table 1. Residues 96 to 106 were omitted from the model in EPi2 and EA because electron density could be identified neither in the open form nor in the closed. The secondary structural elements were used as defined by the program DSSP[20].

Acknowledgements

The authors wish to thank Dr. Peter Sondermann for critical reading of the manuscript. Financial support by EU ERB FMRX-CT98-0204 (M. G.-F.), DFG SPP 1045 (R.H.) and Aventis (T.C.) is acknowledged.

The coordinates of the crystal structures of the PNP synthase complexed forms ES, EPi1, EPi2 and EA have been deposited at the PDB database and are available under accession codes PDB1, PDB2, PDB3 and PDB4, respectively.

REFERENCES

1. Spenser, I. D. & Hill, R. E. (1995). The biosynthesis of pyridoxine. *Nat. Prod. Rep.* **12**, 555-565.
2. Dempsey, W. D. (1987). In *Escherichia coli and Salmonella typhimurium: cellular and molecular biology* (Neidhardt, F. C., Ingraham, J. L., Low, K. B., Magasanik, B., Schaechter, M. & Umbarger, H. E., eds.), pp. 539-543. American Society for Microbiology, Washington, D. C.
3. Yang, Y., Zhao, G. S. & Winkler, M. E. (1996). Identification of the pdxK gene that encodes pyridoxine (vitamin B-6) kinase in Escherichia coli K-12. *FEMS Microbiol. Lett.* **141**(1), 89-95.
4. Cane, D. E., Hsiung, Y. J., Cornish, J. A., Robinson, J. K. & Spenser, I. D. (1998). Biosynthesis of vitamin B-6: The oxidation of 4- (phosphohydroxy)-L-threonine by PdxA. *J. Am. Chem. Soc.* **120**(8), 1936-1937.
5. Cane, D. E., Du, S. & Spenser, I. D. (2000). Biosynthesis of vitamin B6: Origin of the oxygen atoms of Pyridoxol Phosphate. *J. Am. Chem. Soc.* **122**, 4213-4214.
6. Laber, B., Maurer, W., Scharf, S., Stepusin, K. & Schmidt, F. S. (1999). Vitamin B-6 biosynthesis: formation of pyridoxine 5 '-phosphate from 4-(phosphohydroxy)-L-threonine and 1-deoxy-D-xylulose-5- phosphate by PdxA and PdxJ protein. *FEBS Lett.* **449**(1), 45-48.
7. Ehrenshaft, M., Jenns, A. E., Chung, K. R. & Daub, M. E. (1998). SOR1, a gene required for photosensitizer and singlet oxygen resistance in Cercospora fungi, is higly conserved in divergent organisms. *Molecular Cell* **1**(4), 603-609.
8. Ehrenshaft, M., Bilski, P., Li, M. S., Chignell, C. F. & Daub, M. E. (1999). A highly conserved sequence is a novel gene involved in de novo vitamin B6 biosynthesis. *Proc. Natl. Acad. Sci.* **96**, 9374-9378.
9. Bilski, P., Li, M. Y., Daub, M. E., Ehrenshaft, M. & Chignell, C. F. (1999). Antioxidant properties of pyridoxine and its derivatives: quenching of singlet oxygen (1O2). *Free Radical Biology and Medicine* **25S**, 28.
10. Osmani, A. H., May, G. S. & Osmani, S. A. (1999). The extremely conserved pyroA gene of Aspergillus nidulans is required for Pyridoxine synthesis and is required indirectly for resistance to photosensitizers. *J. Biol. Chem.* **274**, 23565-23569.
11. Garrido-Franco, M., Laber, B., Huber, R. & Clausen, T. (2001). Structural basis for the function of pyridoxine 5'-phosphate synthase. *Structure* **9**, 245-253.
12. Brünger, A. T. (1992). XPLOR (Version 3.1) Manual. Yale University Press, New Haven and London.
13. Cane, D. E., Du, S. C., Robinson, J. K., Hsiung, Y. & Spenser, I. D. (1999). Biosynthesis of vitamin B-6: Enzymatic conversion of 1-deoxy-D- xylulose-5-phosphate to pyridoxol phosphate. *J. Am. Chem. Soc.* **121**(33), 7722-7723.
14. Barton, G. J. (1993). ALSCRIPT a tool to format multiple sequence alignments. *Protein Eng.* **6**(1), 37-40.

15. Garrido-Franco, M., Huber, R., Schmidt, F. S., Laber, B. & Clausen, T. (2000). Crystallization and preliminary x-ray crystallographic analysis of PdxJ, the Pyridoxine 5'-phosphate synthesizing enzyme. *Acta Cryst. Sect. D* **56**, 1045-1048.
16. Otwinowski, Z. & Minor, W. (1997). Processing of X-ray diffraction data collected in oscillation mode. *Meth. Enzymol.* **276**, 307-326.
17. Collaborative Computing Project Number 4 (1994). The CCP4 Suite - Programs For Protein Crystallography. *Acta Cryst. Sect. D* **50**, 760-763.
18. Engh, R. A. & Huber, R. (1991). Accurate bond and angle parameters for X-ray protein-structure refinement. *Acta Cryst. Sect. A* **47**, 392-400.
19. Jones, T. A. & Kjelgaard. (1991). O-The Manual. Uppsala, Sweden.
20. Kabsch, W. & Sander, C. (1983). Dictionary of protein secondary structure: pattern recognition of hydrogen bonded and geometrical features. *Biopolymers* **22**, 2577-2637.
21. Kraulis, P. J. (1991). MOLSCRIPT: a program to produce both detailed and schematic plots of protein structures. *J. Appl. Cryst.* **24**, 946-950.
22. Merrit, E. A. & Murphy, M. E. P. (1994). RASTER3D Version 2.0. A program for photorealistic molecular graphics. *Acta Cryst. Sect. D* **50**, 869-873.
23. Evans, S.V. (1993). Setor - Hardware-Lighted 3-Dimensional Solid Model Representations of Macromolecules. *J. Mol. Graph.* **11**, 134-141.